

## Supplementary Information

### Multiplexed Electrical Detection of Whole Viruses from Plasma in a Microfluidic Platform

Aaron Jankelow<sup>1,2,3</sup>, Chih-Lin Chen<sup>4</sup>, Thomas W. Cowell<sup>4</sup>, Javier Espinosa de los Monteros<sup>1,3</sup>, Zheng Bian<sup>1,2</sup>, Victoria Kindratenko<sup>1,2</sup>, Katherine Koprowski<sup>1,2</sup>, Sriya Darsi<sup>1,2</sup>, Hee-Sun Han<sup>4,5</sup>, Enrique Valera<sup>1,2,3,5\*</sup>, Rashid Bashir<sup>1,2,3,5,6,7,8,9\*</sup>

<sup>1</sup> Department of Bioengineering, University of Illinois at Urbana-Champaign, Urbana, IL, 61801, USA

<sup>2</sup> Nick Holonyak Jr. Micro and Nanotechnology Laboratory, University of Illinois at Urbana-Champaign, Urbana, IL, 61801, USA

<sup>3</sup> Biomedical Research Center, Carle Foundation Hospital, Urbana, Illinois, USA

<sup>4</sup> Department of Chemistry, University of Illinois at Urbana-Champaign, Urbana, IL, 61801, USA

<sup>5</sup> Carl R. Woese Institute for Genomic Biology, University of Illinois at Urbana-Champaign, Urbana, Illinois, USA.

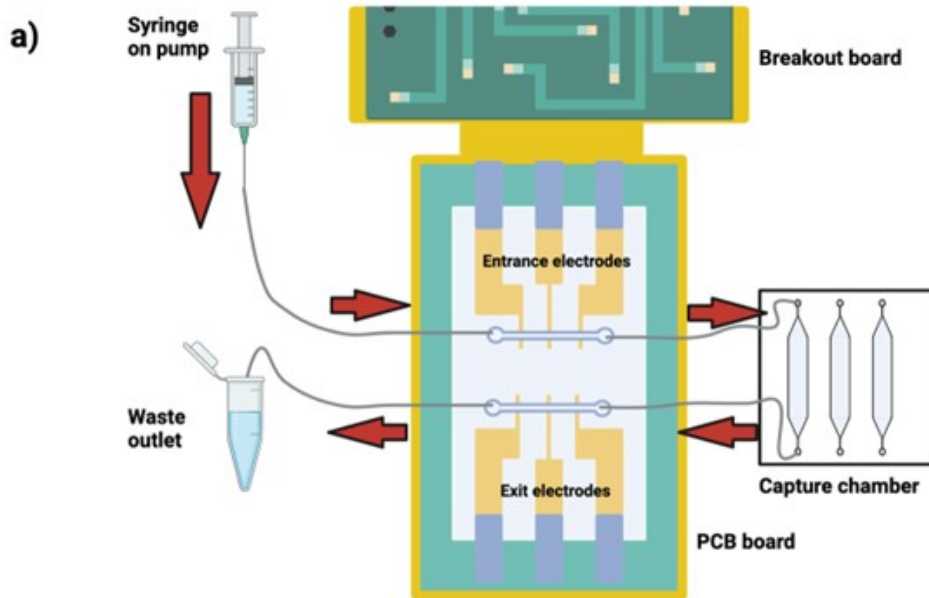
<sup>6</sup> Department of Biomedical and Translation Science, Carle Illinois College of Medicine, University of Illinois at Urbana-Champaign, Urbana, IL, 61801, USA

<sup>7</sup> Department of Electrical and Computer Engineering, University of Illinois at Urbana-Champaign, Urbana, IL, 61801, USA

<sup>8</sup> Department of Mechanical Science and Engineering, University of Illinois at Urbana-Champaign, Urbana, IL, 61801, USA

<sup>9</sup> Department of Materials Science and Engineering, University of Illinois at Urbana-Champaign, Urbana, IL, 61801, USA

\* Corresponding authors: Enrique Valera (evalerac@illinois.edu), Rashid Bashir (rbashir@illinois.edu).



b)



**Figure S1.** Schematic of instrumentation. **a)** Pump is used to inject sample loaded in the syringe at  $20 \mu\text{L}/\text{min}$  into entrance electrode channel. Liquid flows past set of entrance electrodes. Liquid flows from entrance electrode outlet through tubing into one capture chamber from a set of six, where beads will be captured as the flow through. The outlet of the capture chamber connects via tubing to the inlet of the exit electrode channel, which passes through the set of exit electrodes. Both sets of electrodes are connected to a PCB board using silver epoxy, which is inserted by a breakout board connected to the lock-in amplifier. Image created with Biorender. **b)** Photo of lock-in amplifier which is connected to the breakout board.

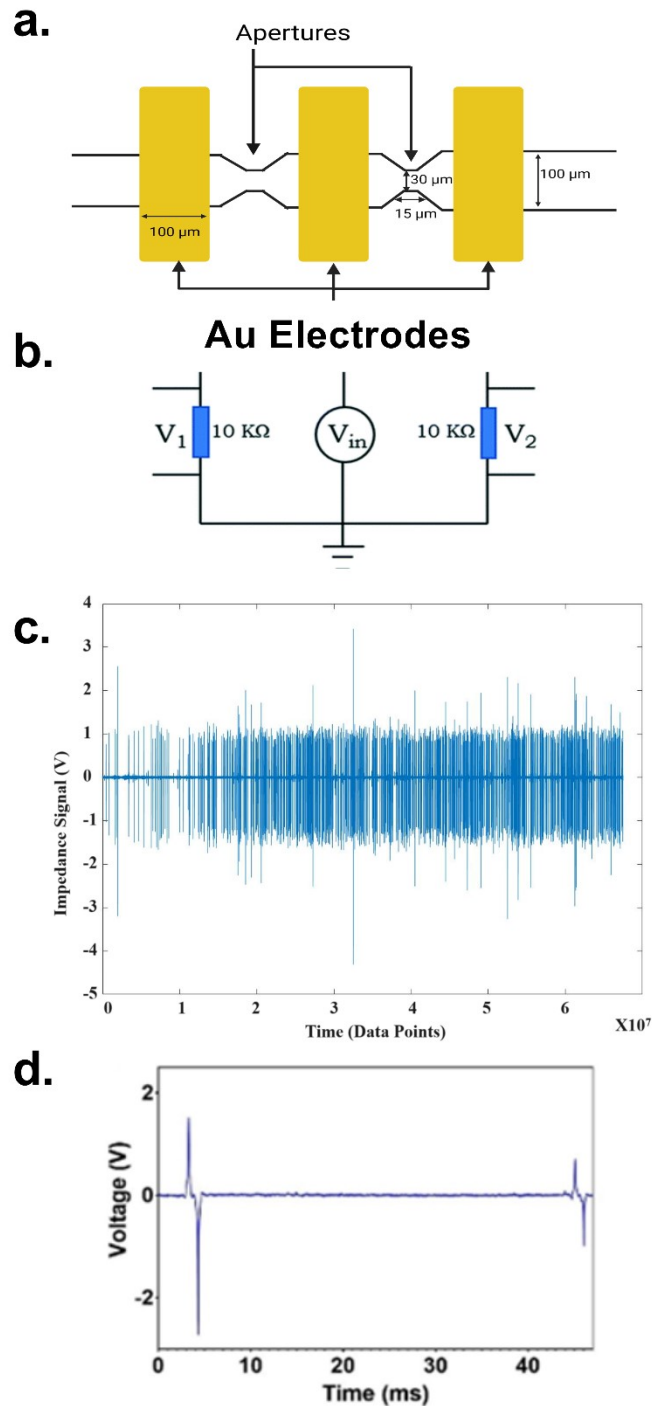


**Figure S2.** Differential electrical counting technology. **a)** Electrodes measure the impedance changes caused by beads flowing through the aperture between the electrodes through the use of a **b)** Wheatstone bridge circuit by acquiring output voltages across a  $10\text{ k}\Omega$  resistor with a sampling rate of  $250\text{ kHz}$  to produce an **c)** impedance over time plot. Within this plot one can identify **d)** individual peaks which can be analyzed for their maximum values via MATLAB which will vary based on the size and composition of the beads used. Images S2a and S2b created with Biorender.

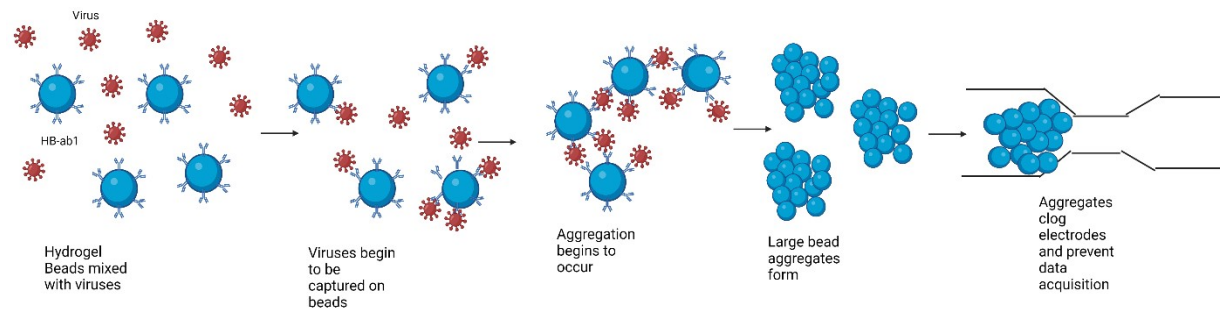


**Figure S3.** Schematic of aggregation when not performing pre-incubation. Hydrogel Beads conjugated to primary antibody are mixed with virus in solution. Because each virus has multiple proteins and each bead has multiple antibodies, one bead can bind to multiple viruses and one virus can lead to multiple beads. Over the incubation period this will lead to increasing amounts of aggregation as beads form complexes with viruses attached to other beads, until many large aggregates are present which can clog electrodes and prevent the proper acquisition of data. Image created with Biorender.

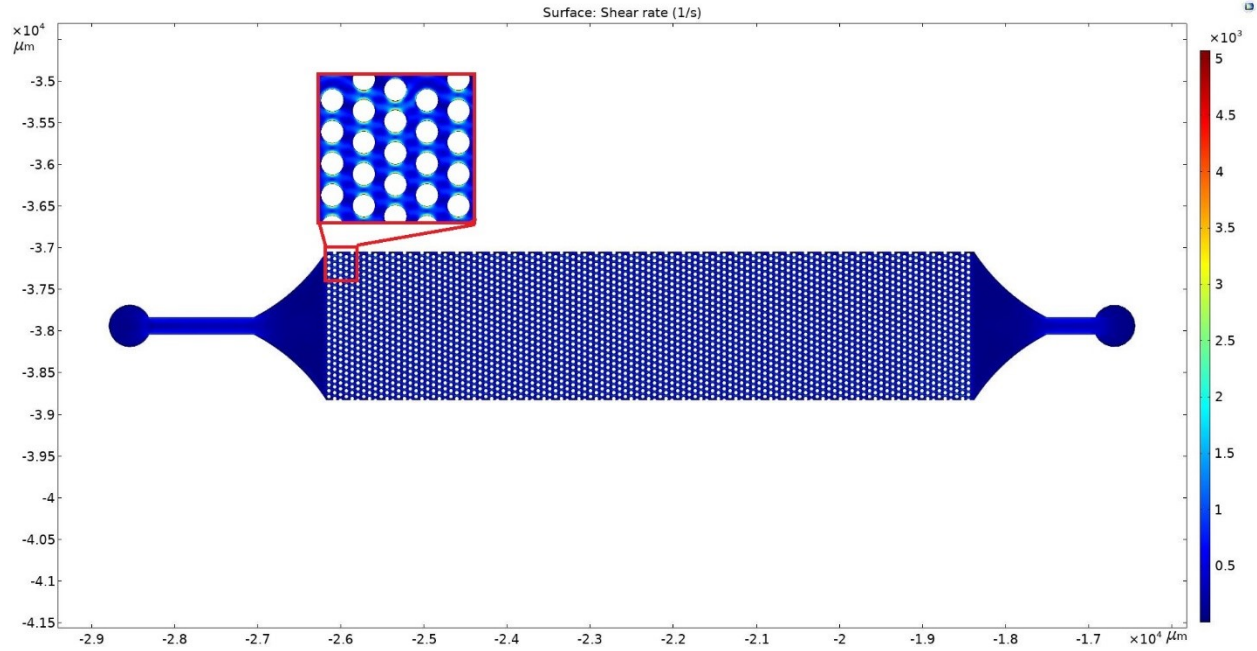
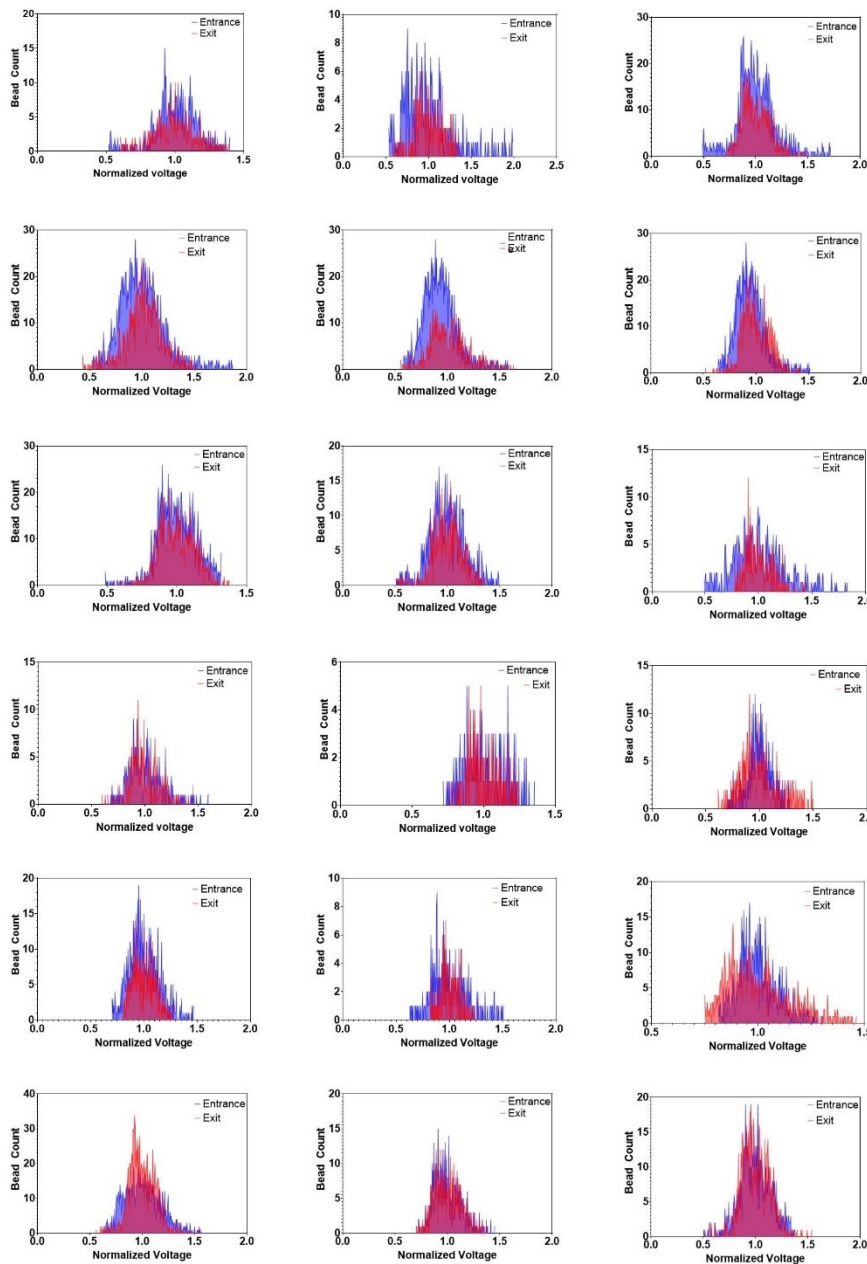


**Figure S4.** COMSOL shear rate simulation of capture chamber. A 2D simulation of the chamber geometry was created by importing geometry from AutoCAD and autogenerating the mesh which contains a total of 775634 elements. A laminar flow analysis was performed with a stationary study. Flow was simulated at  $3.33333\text{e-}10 \text{ m}^3/\text{s}$  ( $20 \text{ }\mu\text{L}/\text{min}$ ) based on a chamber height of  $55 \text{ }\mu\text{m}$ , going from an inlet at the left side to the outlet on the right. Shear Rate around pillars was determined to be at consistent levels with designs used previously (average shear rate around the pillars  $\sim 700 \text{ s}^{-1}$  and a maximum shear rate around the pillars of about  $5000 \text{ s}^{-1}$ ) to allow for similar rates of specific capture.



$2 \times 10^4$  IU/mL

$1 \times 10^4$  IU/mL

$8 \times 10^3$  IU/mL

$4 \times 10^3$  IU/mL

$2 \times 10^3$  IU/mL

0 IU/mL

**Figure S5.** Entrance and exit histograms for HAV individual assay. Voltages are normalized against average voltage signal of counts.

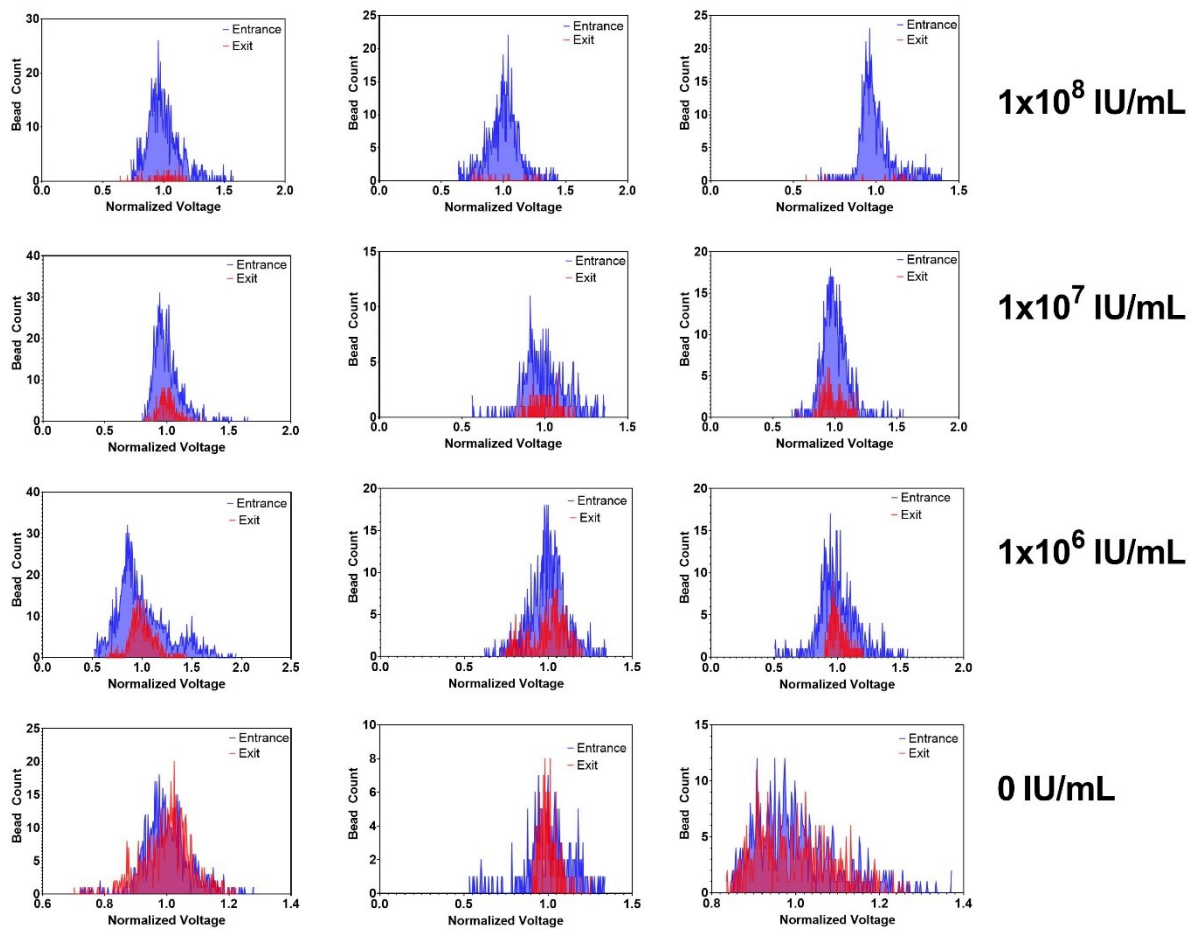


**Figure S6.** Entrance and Exit histograms for B19V individual assay. Voltages are normalized against average voltage signal of counts.

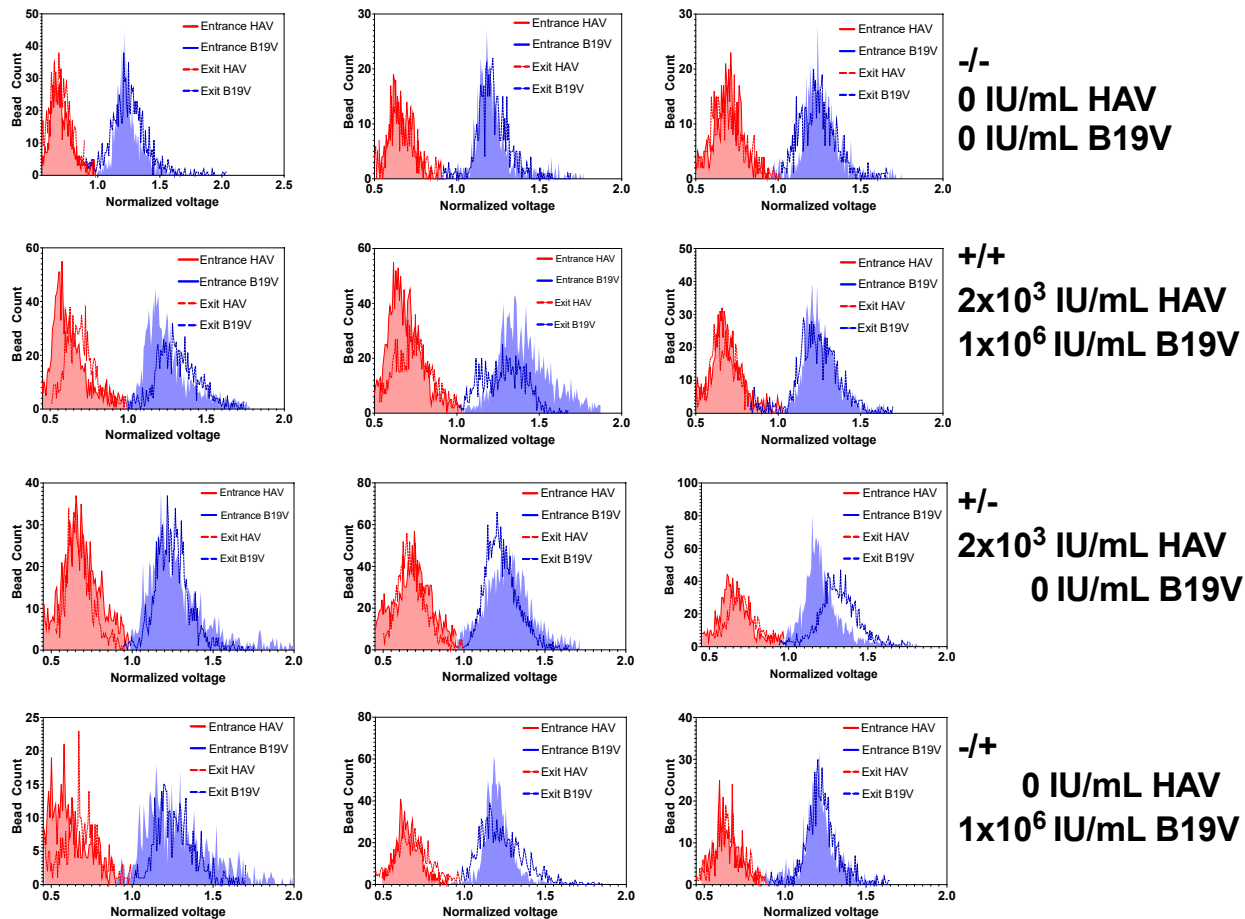


**Figure S7.** Entrance and exit histograms for multiplexed testing. Voltages are normalized against average voltage signal of counts.